JACS Au
AN OPEN ACCESS JOURNAL OF THE AMERICAN CHEMICAL SOCIETY

pubs.acs.org/jacsau
Article

Organocatalyzed Enantioselective C−N Bond-Forming S_NAr Reactions for Synthesizing Stereogenic-at-Boron BODIPYs

Yan-Dong Meng,[†] Wei Fang,[†] Zheng-Hao Pei,[†] Wen-Hao Chen,[†] Shu-Ying Ding, Meng-Lan Shen, Yingcui Bu,* Chuan-Zhi Yao, Qiankun Li, Jie Yu,* and Hua-Jie Jiang*

Cite This: *JACS Au* 2025, 5, 1965−1973

Read Online

ACCESS | Metrics & More | Article Recommendations | Supporting Information

ABSTRACT: The precise construction of boron stereogenic centers represents a significant, yet challenging frontier in asymmetric catalysis, garnering growing attention in recent years. However, feasible catalysis has primarily been limited to transition-metal-catalyzed desymmetrization of pro-chiral BODIPY molecules, while enantioselective synthesis via organocatalysis remains unexplored. Herein, we achieve an organocatalyzed C−N bond-forming SNAr reaction of 3,5-dihalogen BODIPYs via phase-transfer catalysis, enabling the efficient synthesis of a broad range of boron-stereogenic BODIPYs with excellent enantioselectivities (>40 examples, up to 99% ee). The significance and potential of this catalytic approach are further underscored by the versatile applications of enantioenriched 3-amide BODIPYs in asymmetric synthesis, optical activity regulation, bioimaging, and sensing, promoting the development of boron-stereogenic fluorophores.

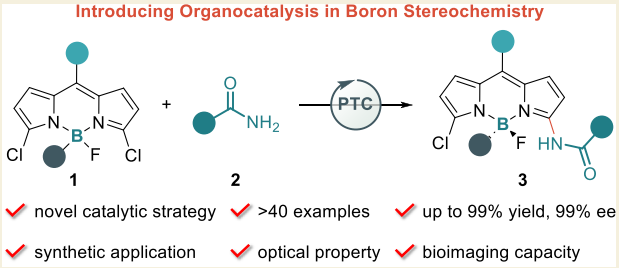

KEYWORDS: *boron-steregenic center, asymmetric S_NAr reaction, organocatalysis*

INTRODUCTION

Chiroptical luminophore-containing molecules, celebrated for their exceptional ability to integrate enantioselectivity with fluorescence, have become invaluable across diverse fields, including chiral sensing, bioimaging, advanced material science, and asymmetric catalysis.[1−3] Among numerous fluorophores, BODIPY (boron dipyrromethene) dyes have been regarded as promising organic fluorophores, prized for their distinctive photophysical properties and the flexibility of their structure, which allows precise modulation of fluorescence behavior.[4−8] Specifically, through rational functional modification, boron-centered chiral BODIPY derivatives demonstrate microenvironment-responsive characteristics in biological systems, enabling real-time visualization of dynamic cellular processes.[9] Furthermore, these stereoselective compounds can selectively respond to biological targets, which largely improves the precision of fluorescence imaging-guided disease diagnosis.[10−12] Over the past decades, various chiral BODIPY dyes have been developed, with their exceptional optical properties underscoring their widespread applications in chiral optoelectronic materials (Scheme 1A).[13,14] However, synthesizing chiral BODIPY dyes and their analogues has largely relied on incorporating chiral modules into the BODIPY structure or chiral HPLC separation, and using asymmetric catalysis for their precise synthesis remains highly limited.[15−23] Moreover, the catalytic enantioselective synthesis of chiral BODIPYs containing B-chirality[13,24,25] presents a significant challenge, with rare successful cases (Scheme 1B). In 2021, He and co-workers unveiled an unprecedented catalytic enantioselective synthesis of stereogenic-at-boron BODIPY dyes via copper-catalyzed click reactions.[26] Song groups demonstrated that Cu-catalyzed asymmetric B−H carbene insertion reactions were effective protocols for synthesizing chiral organoboranes.[27] In 2023, the He group reported a Pd-catalyzed intramolecular C−H arylation reaction, accessing a diverse array of enantioenriched boron heterocycle-containing BODIPYs.[28] Very recently, they developed a modular assembling strategy to address this issue via Pd-catalyzed Suzuki coupling[29] and Buchwald coupling reactions.[30] During our manuscript preparation, Wang and co-workers exhibited an enantioselective Rh-catalyzed C−H arylation reaction, delivering (axially) boron-stereogenic BODIPY dyes with excellent stereocontrol.[31]

Despite these notable advances, developing novel catalysis for synthesizing structurally diverse boron-stereogenic BODIPY dyes is still essential, given their unique photophysical properties and promising applications. Moreover, to our knowledge, the organocatalyzed enantioselective synthesis of boron-stereogenic BODIPYs has yet to be explored, and organocatalysis undoubtedly will inject new impetus into chiral BODIPY

Received: February 19, 2025
Revised: March 24, 2025
Accepted: March 26, 2025
Published: April 2, 2025

https://doi.org/10.1021/jacsau.5c00196
JACS Au 2025, 5, 1965−1973

Scheme 1. Chiral BODIPY Dyes and Catalytic Synthesis of Stereogenic-at-Boron BODIPYs. (A) Representative Examples of Chiral BODIPY Dyes; (B) TM-Catalyzed Synthesis of Stereogenic-at-Boron BODIPYs; and (C) This Work: Organocatalyzed Enantioselective C−N Bond-Forming S_NAr Reactions for Accessing Stereogenic-at-Boron BODIPYs

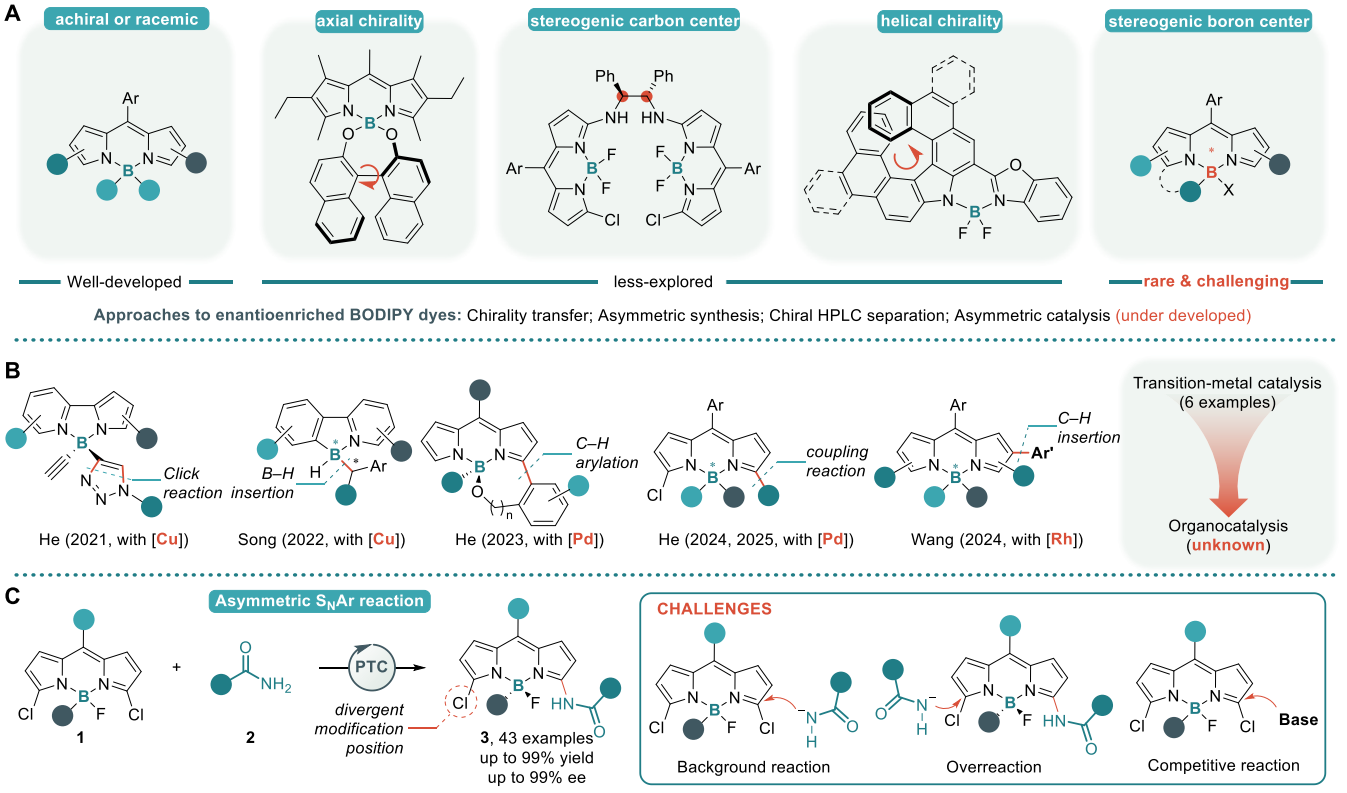

synthesis. Asymmetric phase-transfer catalysis has become one of the most renowned and successful strategies in organocatalysis over the past decades.[32−39] Notably, it has proven to be an effective approach for tackling the challenging enantioselective nucleophilic aromatic substitution (S_NAr) reactions, enabling the enantioselective α-arylation of enolates and *O*-arylation of (*o*-hydroxy)aryl-alkene aldehydes.[40−48] In this protocol, an electron-deficient aryl fluoride is the key in accelerating the substitution process. Given the strong Lewis acidity of B(III) atoms,[49−54] which significantly enhances molecular electrophilicity, 3,5-halogens BODIPYs could be excellent substrates for asymmetric S_NAr reactions with nucleophiles (Scheme 1C).[29,55−59] In this scenario, several obstructions should be addressed: (1) the strong electrophilicity of BODIPYs leads to noncatalytic background reactions, providing racemic products; (2) the overreaction results in achiral byproducts; and (3) the base serves as a nucleophile, bringing competitive reactions. Herein, we report a catalytic asymmetric synthesis of stereogenic-at-boron BODIPY dyes via phase-transfer-catalyzed C−N bond-forming S_NAr reactions, leading to a diverse range of enantioenriched α-amide BODIPYs (41 examples, up to 99% yield, up to 99% ee). These unique stereogenic-at-boron dyes could serve as ideal platform molecules facilitating the stereospecific transformation into structurally diverse chiral BODIPYs and their photophysical properties and bioapplications hold significant potential for materials science.

RESULTS AND DISCUSSION

Our investigation commenced with the asymmetric S_NAr reaction between 3,5-Cl_2 BODIPY **1a** and benzamides (**2a**) in the presence of quinine-derived phase-transfer catalyst **PTC-1** and KOH as bases. To our delight, the stereogenic-at-boron 3-amide BODIPY **3a** was obtained with 79% yield and 86% ee by using toluene as solvent (Table 1, entry 1, for details, see Table S1 in Supporting Information). The reaction worked smoothly in DCM, furnishing **3a** in 95% yield with 89% ee (entry 2), but a lot of undetermined byproducts occurred by using $CHCl_3$, albeit the improved enantioselectivity of **3a** was obtained (entry 3). The strong base was crucial for the S_NAr reaction, and even no product could be detected by using LiOH instead of KOH (entries 4, 5). Subsequently, we evaluated the substituent effect of PTCs (entries 6−10). In general, the employment of the PTCs with electron-withdrawing aryl groups enabled excellent stereocontrol and notably, using **PTC-5**, assembling between quinine and pentafluorobenzyl bromide, provided **3a** with 99% ee in moderate yields because of the generation of byproducts (entry 9). Fortunately, both excellent yield and enantioselectivity of **3a** were obtained in the presence of **PTC-6**, featuring with 3,5-$(CF_3)_2$ benzyl groups (entry 10). At last, the optimal reaction condition was obtained by decreasing the reaction temperature to −25 °C, delivering 3-amide BODIPY **3a** in 93% yield with 97% ee (entry 12).

With the optimized reaction conditions in hand, we explored the substrate scope of asymmetric S_NAr reactions (Scheme 2). In general, a board of amides was well tolerated in the reaction system. For instance, the reactions worked smoothly by using various electron-rich or poor 4-substituted aryl amides as nucleophiles, furnishing the corresponding stereogenic-at-boron BODIPY dyes **3a**−**3i** with excellent enantioselectivities (>92% ee). Notable, subjecting 4-nitrobenzamides into the reaction delivered product **3i** in 93% yield with 99% ee. The absolute

https://doi.org/10.1021/jacsau.5c00196
JACS Au 2025, 5, 1965−1973

Table 1. Optimization of the Reaction Conditions[a]

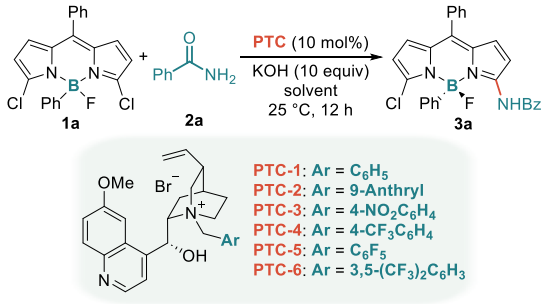

entry	PTC	solvent	yield (%)	ee (%)
1	**PTC-1**	toluene	79	86
2	**PTC-1**	DCM	95	88
3	**PTC-1**	$CHCl_3$	67	92
4[b]	**PTC-1**	DCM	84	85
5[c]	**PTC-1**	DCM	0	N.D.
6	**PTC-2**	DCM	65	81
7	**PTC-3**	DCM	96	89
8	**PTC-4**	DCM	90	88
9	**PTC-5**	DCM	47	99
10	**PTC-6**	DCM	99	94
11[d]	**PTC-6**	DCM	94	96
12[e]	**PTC-6**	**DCM**	**93**	**97**
13[f]	**PTC-6**	DCM	99	95

[a]Unless otherwise specified, all reactions were carried out using **1a** (0.10 mmol), **2a** (0.20 mmol), **PTC** (10 mol %), and KOH (1.0 mmol, power) in solvent (1.0 mL) at 25 °C for 12 h. Isolated yield was given and the enantiomeric excess (ee) was determined by HPLC. N.D. = not detected. [b]NaOH was used instead of KOH. [c]LiOH was used instead of KOH. [d]Reaction was performed at −20 °C. [e]Reaction was performed at −25 °C. [f]Reaction was performed at −30 °C for 36 h.

configuration of enantioenriched **3a** was determined via X-ray crystallographic analysis (CCDC 2418773). Various 3-substituted aryl amides were all compatible under optimal conditions with 96% ee in satisfactory yields (**3m**−**3o**). Next, we evaluated the amide nucleophiles containing a multisubstituted aryl (**3p**), polycyclic aryl (**3q**), and heterocycles (**3r**−**3u**), allowing an array of chiral conditions (**3j**−**3l**) and importantly, using sterically hindered 2-substituted aryl amines also afforded stereogenic-at-boron BODIPYs to be obtained with excellent yields and enantioselectivities (>94% ee). To our delight, alkyl amides were also ideal nucleophiles, leading to outstanding yields and stereoselectivities of products **3v**−**3z**. Interestingly, our protocol was well accommodated with enamides and ynamides, highlighting good functional group tolerance (**3aa**−**3ac**). Carbamates and sulfoximines were also well tolerated in our reaction system, delivering corresponding chiral BODIPY **3ad** in 88% yield with 97% ee and **3ae** in 89% yield with 97% ee, respectively. Subsequently, we investigated the generality of our approach concerning 3,5-Cl_2 BODIPY scaffolds. The enantioselective S_NAr reactions of BODIPYs bearing various aryl substituents at the *meso* position worked smoothly, delivering the corresponding enantioenriched 3-amide-BODIPYs in excellent yields with enantioselectivities up to 96% ee (**3af**−**3ak**). It is worth mentioning that the influence of the substituents on the boron atom was minimal on stereocontrol, furnishing desired chiral 3-amide BODIPYs **3al**−**3aq** with excellent enantioselectivities. Notably, the BODIPY containing two groups with extremely similar steric hindrance (Me and F) on boron atoms (**1aq**) was perfectly accommodated in the S_NAr reaction with excellent stereoselectivity (**3aq**), implying that stereocontrol could not be ascribed to the steric difference between the two substituents on boron atoms (for proposed preliminary asymmetric induction model, see Section 7 in Supporting Information).

Next, we investigated the synthetic application of stereogenic-at-boron BODIPYs. A gram-scale reaction with **1a** was carried out first, delivering chiral product **3a** without significant erosion of both the yield and enantioselectivity (1.27 g, 88% yield, 96% ee, Scheme 3A). To our delight, the second S_NAr reaction of enantioenriched **3a** with 4-(*tert*-butyl) benzenethiol worked smoothly in the presence of **PTC-6**, affording stereogenic-at-boron BODIPY **4** in 84% yield with 95% ee. Although extensive efforts toward the second S_NAr reaction with *N*-nucleophiles were unsuccessful due to the decreased electrophilicity of **3a**, the Pd-catalyzed Buchwald coupling reactions between **3a** and 4OMe-$C_6H_4NH_2$ enabled the enantiospecific synthesis of chiral BODIPY **5** in high yields. Moreover, the boron-stereogenic BODIPY bearing a β-naphthyl (**6**) or alkynyl (**7**) was easily obtained via the Suzuki coupling or Sonogashira coupling reaction, respectively. As a classic fluorescence probe, the photophysical properties of selected boron-stereogenic BODIPY dyes (**3l**, **3p**, **3t**, **3w**, **3ab**, **3ah**, and **3an**) were subsequently evaluated. As shown in Scheme 3B, the normalized absorption spectra of selected BODIPY dyes revealed ∼20 nm of bathochromic shift at maximum absorption wavelength by the fine adjustment of lateral groups. Meanwhile, all of them displayed efficient radiative transitions with wide fluorescence emissions in the range of 520 to 650 nm (Scheme 3C), which can ensure promising biological applications.[60] Further, the chiroptical properties of representative BODIPY derivants were investigated in the solution state by circular dichroism (CD) and a circular polarized luminescence (CPL) spectroscope. The CD spectra exhibited obvious peaks at ∼330 and ∼530 nm, respectively (Scheme 3D), verifying the similar chiroptical activity of the derivants **31** and **3ab**. Also, enantiomers (*R*)-**3u** and (*S*)-**3u** displayed intense CPL signals at ∼590 nm when dispersed in a toluene solution, higher than the most reported organic fluorescence systems (Scheme 3E). To further demonstrate that they are monodisperse rather than aggregated in a toluene solution, transmission electron microscopy was utilized to visualize their morphology and size. Taking (*R*)-**3u** for example, no obvious particles can be observed (for details, see Figure S2 in Supporting Information). Overall, the BODIPY dye platform combines glorious optical gains and chiroptical activity, making it a suitable candidate in the fields of luminous material and biological medicinal application as well.[19,29,61]

In view of the excellent emission performance in vitro, we then investigated the fluorescence imaging ability at the cellular level. First, a series of typical stereogenic-at-boron BODIPYs, such as **3l**, **3w**, **3ab**, **3p**, **3t**, **3ah**, and **3an** were elaborately selected to coincubate with HepG2 cells for 10 min, respectively. After the cells were washed with PBS buffer, confocal laser scanning microscopy was immediately utilized for visualization. As depicted in Figure 1A, upon excitation at ∼510 nm, the bright fluorescence signals collected in the range of 540 to 560 nm presented inhomogeneous punctate distribution (Enlarged Area) in all groups (**3l**, **3w**, **3ab**, **3p**, **3t**, **3ah** and **3an**), which indicated their superior bioimaging capacity. Further, to confirm the specific spatial distribution of BODIPY derivatives in HepG2 cells, colocalization imaging experiments using four commercial cellular markers were carried out in succession: (i) DAPI for

https://doi.org/10.1021/jacsau.5c00196
JACS Au 2025, 5, 1965−1973

Scheme 2. Substrate Scope of Asymmetric S_NAr Reactions[a]

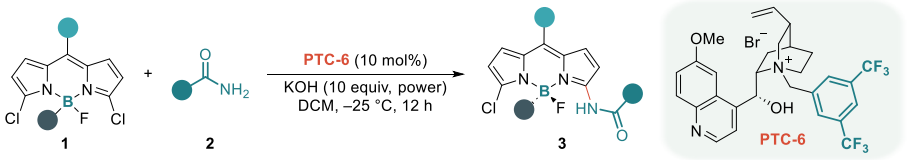

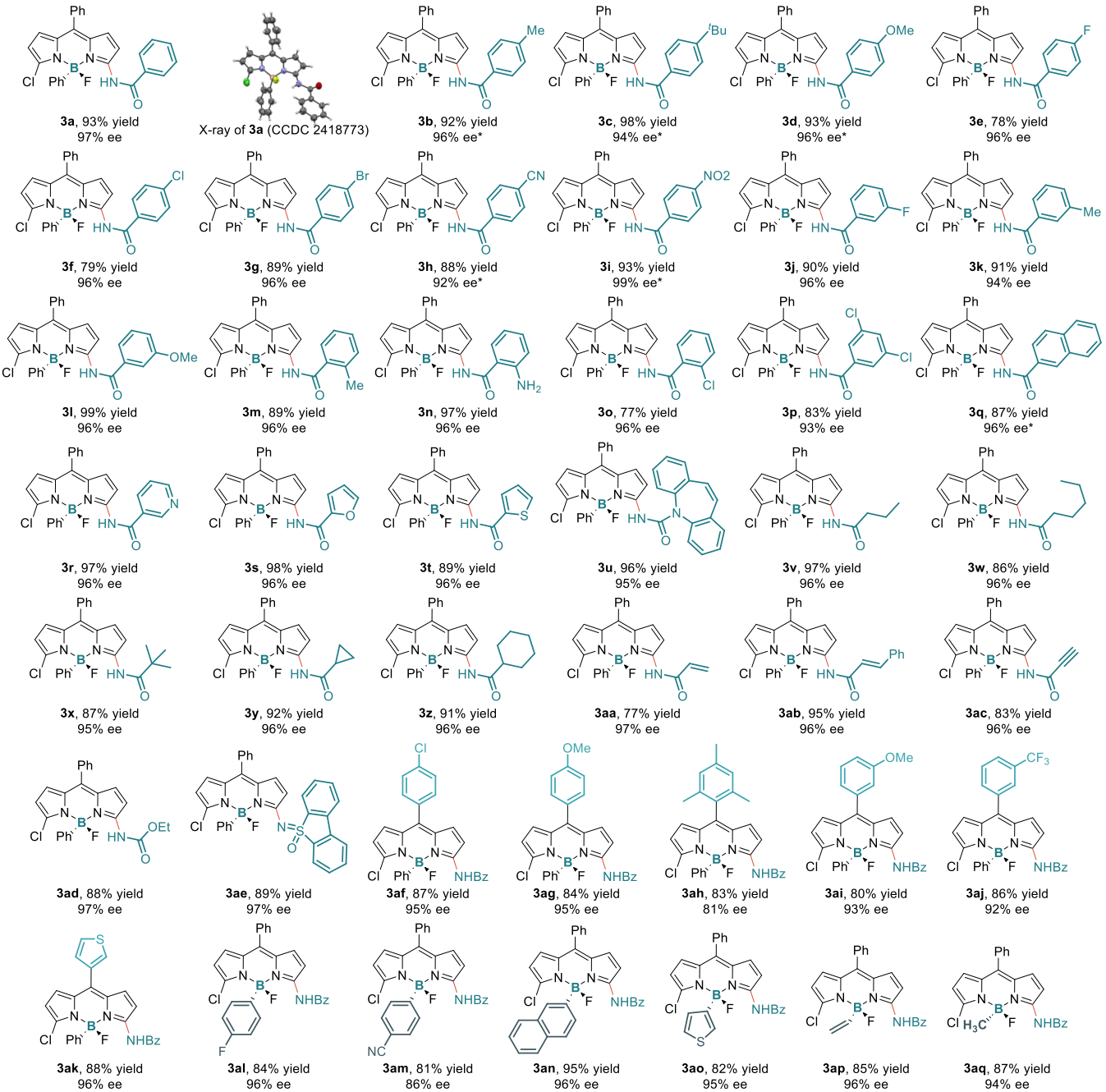

[a]Unless otherwise specified, all reactions were carried out using **1** (0.10 mmol), **2** (0.20 mmol), **PTC-6** (10 mol %), and KOH (1.0 mmol, power) in DCM (1.0 mL) at −25 °C for 12 h. Isolated yield was given and the enantiomeric excess (ee) was determined by HPLC. * The reaction was performed at −10 °C.

nucleic acid, (ii) LysoTracker Deep Red for lysosome, (iii) MitoTracker Deep Red for mitochondria, and (iv) LipiDye for lipid droplets. Taking **3an** for example, the merged images as illustrated in Figure 1B, revealed that the evident spherical spot morphologies of **3an** overlapped very well with LipiDye dye dealt cells, during which the Pearson's coefficients (Pr) was calculated to be as high as 0.81. Conversely, the dotted fluorescence of **3an** barely merged with the emission signals of DAPI (Pr = −0.03), MitoTracker Deep Red (Pr = 0.12), and LysoTracker Deep Red (Pr = 0.40).[62−65] The above results

https://doi.org/10.1021/jacsau.5c00196
JACS Au 2025, 5, 1965−1973

Scheme 3. Synthetic Applications and Optical Properties. (A) Gram-Scale Reaction and Post-Modification of Stereogenic-at-Boron BODIPY 3a; (B) Normalized Absorption Spectra; (C) Fluorescence spectra; (D) CD Spectra of 3l and 3ab; and (E) CPL Spectra of 3u. The Normalized Absorption and Fluorescence Spectra of 10 μM Selected BODIPYs in Dimethyl Sulfoxide Solution (λ_{ex} = 520 nm); the CD Spectra of 10 μM 31 and 3ab in Methanol Solution; and the CPL Spectra of 10 μM (*R*)-3u and (*S*)-3u in a Toluene Solution (λ_{ex} = 390 nm)

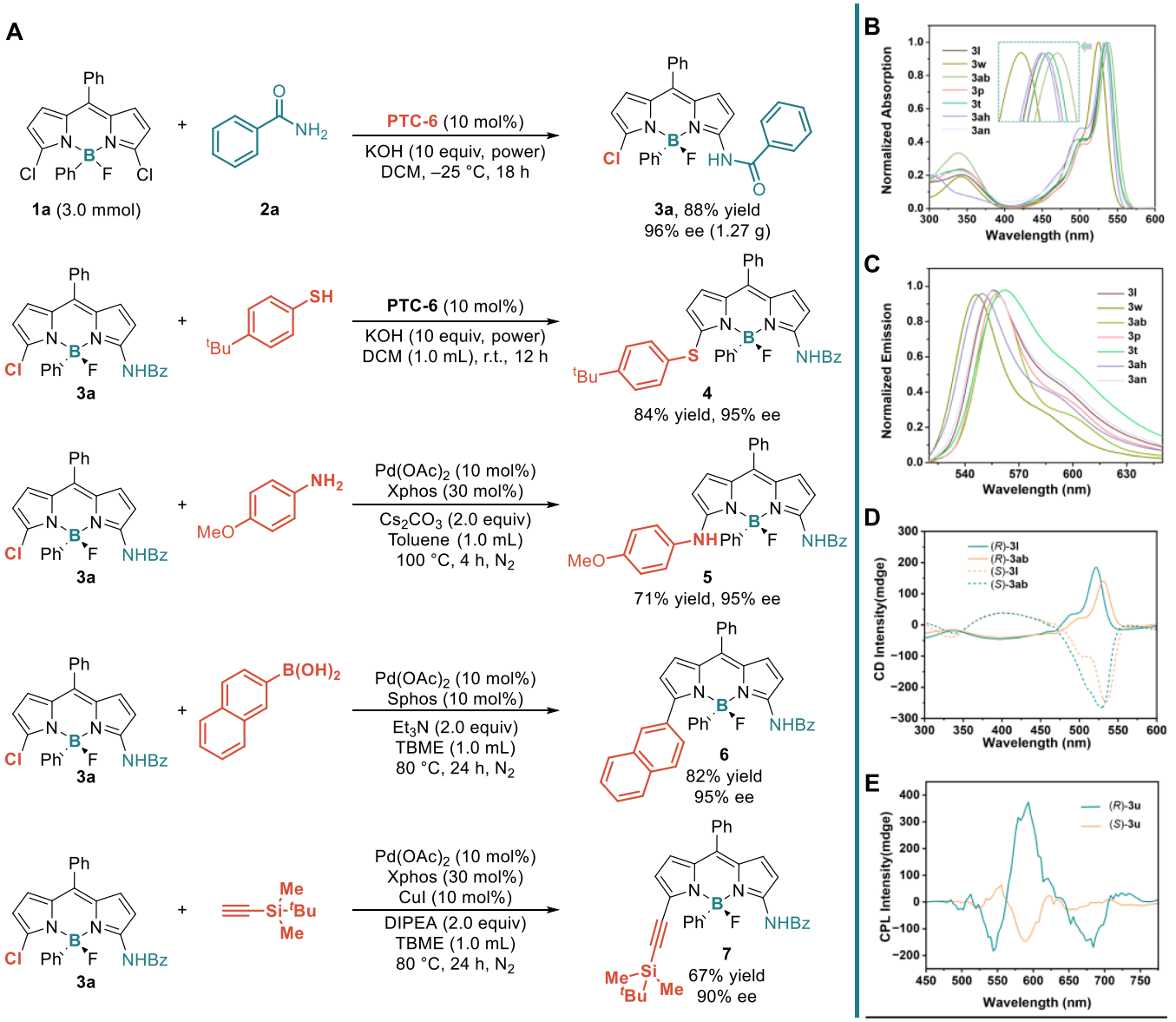

demonstrated that the as-prepared BODIPY could precisely localize in the lipid droplets, presenting a promising prospect for real-time monitoring of liposome-related physiological and pathological activities.

CONCLUSIONS

In summary, we have developed an efficient organocatalyzed asymmetric C–N bond-forming S_NAr reaction of pro-chiral BODIPYs via phase-transfer catalysis, enabling a broad range of stereogenic-at-boron fluorescent molecules with excellent enantioselectivities (>40 examples, up to 99% ee). Notably, substrates with minimal steric differences (Me and F) were also well tolerated, underscoring the exceptional stereocontrol offered by our protocol. The significance and potential of this catalytic approach are further demonstrated by the versatile applications of enantioenriched 3-amide BODIPYs in asymmetric synthesis, optical gain, chiroptical activity, and bioimaging. The organocatalyzed S_NAr reaction paves a distinctive avenue for the precise construction of stereogenic-at-boron molecules, and the novel fluorophores developed in this study hold promise for advancing the discovery and development of chiral luminous materials.

METHODS

General Procedure for the Synthesis of Stereogenic-at-Boron BODIPYs 3a–3aq

An oven-dried 10 mL tube equipped with a magnetic stirring bar was charged with 3,5-Cl_2 BODIPY **1** (0.10 mmol), **PTC-6** (0.01 mmol, 10 mol %), and KOH (10 equiv, power). After adding DCM (1.0 mL), the mixture was cooled to −25 °C and stirred for 30 min. The amide solid **2** (0.20 mmol, 2.0 equiv) was poured into the tube all at once, and the reaction mixture was stirred at −25 °C for 12 h. The mixture was filtered

https://doi.org/10.1021/jacsau.5c00196
JACS Au 2025, 5, 1965–1973

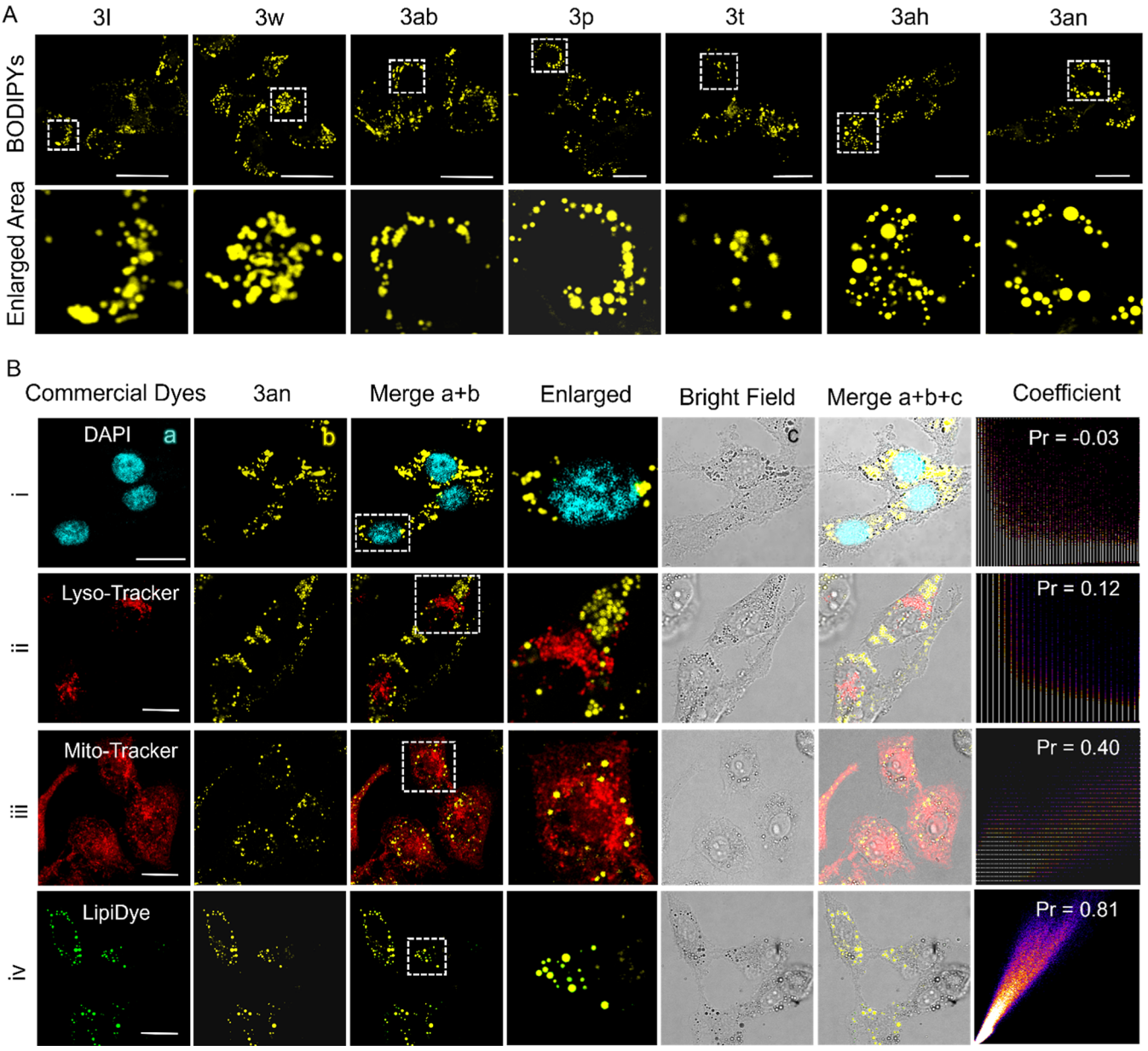

Figure 1. Superior bioimaging capacity. (A) Confocal fluorescence images of HepG2 cells incubated with 10 μM of **3l**, **3w**, **3ab**, **3p**, **3t**, **3ah**, and **3an**, respectively; square dashed box: enlarged images ($\lambda_{ex}/\lambda_{em}$ = 520 nm/540 ~ 570 nm). (B) The colocalization experiments of **3an** and various suborganelle tracker in living HepG2 cells: (i) DAPI ($\lambda_{ex}/\lambda_{em}$ = 405 nm/454 ~ 461 nm), (ii) LysoTracker Deep Red ($\lambda_{ex}/\lambda_{em}$ = 647 nm/668 nm), (iii) MitoTracker Deep Red ($\lambda_{ex}/\lambda_{em}$ = 644 nm/665 nm), and (iv) LipiDye ($\lambda_{ex}/\lambda_{em}$ = 405 nm/521 ~ 530 nm); scale bars: 20 μm.

through a short pad of silica gel (eluent: DCM), and the filtrate was concentrated. The residue was purified by silica gel chromatography using petroleum ether/dichloromethane = 3:1 to afford enantioenriched products **3a**–**3aq**.

Cell Culture and Fluorescence Imaging

HepG2 cells were cultured in cell culture dishes with Dulbecco's modified Eagle's medium containing 10% fetal bovine serum and incubated in an air atmosphere (37°, 5% CO_2). For fluorescence imaging, the cells were planted into glass bottom dishes (15 × 15 mm) at a density of 104 to 106.

Colocalization Experiments

Briefly, HepG2 cells were incubated with the as-prepared BODIPY (5 μM) for 10 min and then treated with various commercial markers (1 μM) for another 15 min. Afterward, the cells were washed with PBS three times, which were viewed immediately on a confocal laser scanning microscope.

■ ASSOCIATED CONTENT

Supporting Information

The Supporting Information is available free of charge at https://pubs.acs.org/doi/10.1021/jacsau.5c00196.

Experimental procedures, spectroscopic data of compounds, X-ray crystal structure data for **3a**, and computational details (PDF)

Accession Codes

CCDC 2285873 contains the supplementary crystallographic data for this paper. These data can be obtained free of charge via www.ccdc.cam.ac.uk/data_request/cif, by emailing data_request@ccdc.cam.ac.uk, or by contacting The Cambridge Crystallographic Data Centre, 12 Union Road, Cambridge CB2 1EZ, UK; fax: 441223 336033.

https://doi.org/10.1021/jacsau.5c00196
JACS Au 2025, 5, 1965−1973

AUTHOR INFORMATION

Corresponding Authors

Yingcui Bu − *Department of Applied Chemistry, Anhui Province Engineering Laboratory for Green Pesticide Development and Application, and Anhui Province Key Laboratory of Crop Integrated Pest Management, Anhui Agricultural University, Hefei 230036, China*; Email: byc@ahau.edu.cn

Jie Yu − *Department of Applied Chemistry, Anhui Province Engineering Laboratory for Green Pesticide Development and Application, and Anhui Province Key Laboratory of Crop Integrated Pest Management, Anhui Agricultural University, Hefei 230036, China*; orcid.org/0000-0002-9968-1429; Email: jieyu@ustc.edu.cn

Hua-Jie Jiang − *Department of Applied Chemistry, Anhui Province Engineering Laboratory for Green Pesticide Development and Application, and Anhui Province Key Laboratory of Crop Integrated Pest Management, Anhui Agricultural University, Hefei 230036, China*; orcid.org/0000-0001-5165-5072; Email: jianghj@ahau.edu.cn

Authors

Yan-Dong Meng − *Department of Applied Chemistry, Anhui Province Engineering Laboratory for Green Pesticide Development and Application, and Anhui Province Key Laboratory of Crop Integrated Pest Management, Anhui Agricultural University, Hefei 230036, China*

Wei Fang − *Department of Applied Chemistry, Anhui Province Engineering Laboratory for Green Pesticide Development and Application, and Anhui Province Key Laboratory of Crop Integrated Pest Management, Anhui Agricultural University, Hefei 230036, China*

Zheng-Hao Pei − *Department of Applied Chemistry, Anhui Province Engineering Laboratory for Green Pesticide Development and Application, and Anhui Province Key Laboratory of Crop Integrated Pest Management, Anhui Agricultural University, Hefei 230036, China*

Wen-Hao Chen − *Department of Applied Chemistry, Anhui Province Engineering Laboratory for Green Pesticide Development and Application, and Anhui Province Key Laboratory of Crop Integrated Pest Management, Anhui Agricultural University, Hefei 230036, China*

Shu-Ying Ding − *Department of Applied Chemistry, Anhui Province Engineering Laboratory for Green Pesticide Development and Application, and Anhui Province Key Laboratory of Crop Integrated Pest Management, Anhui Agricultural University, Hefei 230036, China*

Meng-Lan Shen − *Department of Applied Chemistry, Anhui Province Engineering Laboratory for Green Pesticide Development and Application, and Anhui Province Key Laboratory of Crop Integrated Pest Management, Anhui Agricultural University, Hefei 230036, China*

Chuan-Zhi Yao − *Department of Applied Chemistry, Anhui Province Engineering Laboratory for Green Pesticide Development and Application, and Anhui Province Key Laboratory of Crop Integrated Pest Management, Anhui Agricultural University, Hefei 230036, China*; orcid.org/0000-0003-3518-8114

Qiankun Li − *Department of Applied Chemistry, Anhui Province Engineering Laboratory for Green Pesticide Development and Application, and Anhui Province Key Laboratory of Crop Integrated Pest Management, Anhui Agricultural University, Hefei 230036, China*; orcid.org/0000-0002-4826-1926

Complete contact information is available at: https://pubs.acs.org/10.1021/jacsau.5c00196

Author Contributions

†Y.-D.M., W.F., Z.-H.P., and W.-H.C. contributed equally.

Notes

The authors declare no competing financial interest.

ACKNOWLEDGMENTS

We are grateful for the financial support from NSFC (grants 92156022, 22401004, and 22405005), Anhui Provincial Natural Science Funds (grants 2308085MB43 and 2308085QB44), Shennong Scholar Program of Anhui Agricultural University, and National Undergraduate Training Program for Innovation and Entrepreneurship. The authors acknowledge the assistance provided by the Key Laboratory of Agricultural Sensors, Ministry of Agriculture and Rural Affairs in the photophysical property investigation.

REFERENCES

(1) Pop, F.; Zigon, N.; Avarvari, N. Main-Group-Based Electro- and Photoactive Chiral Materials. *Chem. Rev.* **2019**, *119*, 8435−8478.

(2) Albano, G.; Pescitelli, G.; Bari, D. L. Chiroptical Properties in Thin Films of π-Conjugated Systems. *Chem. Rev.* **2020**, *120*, 10145−10243.

(3) Chen, Y. Circularly polarized luminescence based on small organic fluorophores. *Mater. Today Chem.* **2022**, *23*, 100651−100669.

(4) Loudet, A.; Burgess, K. BODIPY Dyes and Their Derivatives: Syntheses and Spectroscopic Properties. *Chem. Rev.* **2007**, *107*, 4891−4932.

(5) Ulrich, G.; Ziessel, R.; Harriman, A. The Chemistry of Fluorescent Bodipy Dyes: Versatility Unsurpassed†. *Angew. Chem., Int. Ed.* **2008**, *47*, 1184−1201.

(6) Bañuelos, J. BODIPY Dye, the Most Versatile Fluorophore Ever. *Chem. Rec.* **2016**, *16*, 335−348.

(7) Boens, N.; Verbelen, B.; Ortiz, M. J.; Jiao, L.; Dehaen, W. Synthesis of BODIPY dyes through postfunctionalization of the boron dipyrromethene core. *Coord. Chem. Rev.* **2019**, *399*, 213024−213108.

(8) Nguyen, V. N.; Ha, J.; Cho, M.; Li, H.; Swamy, K. M. K.; Yoon, J. Recent developments of BODIPY-based colorimetric and fluorescent probes for the detection of reactive oxygen/nitrogen species and cancer diagnosis. *Coord. Chem. Rev.* **2021**, *439*, 213936−213952.

(9) Liu, H.; Song, W.; Gröninger, D.; Zhang, L.; Lu, Y.; Chan, K. S.; Zhou, Z.; Rurack, K.; Shen, Z. Real-time monitoring of newly acidified organelles during autophagy enabled by reaction-based BODIPY dyes. *Commun. Biol.* **2019**, *2*, 442.

(10) Domaille, D. W.; Zeng, L.; Chang, C. J. Visualizing Ascorbate-Triggered Release of Labile Copper within Living Cells using a Ratiometric Fluorescent Sensor. *J. Am. Chem. Soc.* **2010**, *132*, 1194−1195.

(11) Dodani, S. C.; Leary, S. C.; Cobine, P. A.; Winge, D. R.; Chang, C. J. A Targetable Fluorescent Sensor Reveals That Copper-Deficient *SCO1* and *SCO2* Patient Cells Prioritize Mitochondrial Copper Homeostasis. *J. Am. Chem. Soc.* **2011**, *133*, 8606−8616.

(12) Er, J. C.; Leong, C.; Teoh, C. L.; Yuan, Q.; Merchant, P.; Dunn, M.; Sulzer, D.; Sames, D.; Bhinge, A.; Kim, D.; Kim, S.-M.; Yoon, M.-H.; Stanton, L. W.; Je, S. H.; Yun, S.-W.; Chang, Y.-T. NeuO: a Fluorescent Chemical Probe for Live Neuron Labeling. *Angew. Chem., Int. Ed.* **2015**, *54*, 2442−2446.

(13) Guo, Y.; Zu, B.; Chen, D. C.; He, C. Boron-Stereogenic Compounds: Synthetic Developments and Opportunities. *Chin. J. Chem.* **2024**, *42*, 2401−2411.

(14) Nowak-Król, A.; Geppert, P. T.; Naveen, K. R. Boron-containing helicenes as new generation of chiral materials: opportunities and challenges of leaving the flatland. *Chem. Sci.* **2024**, *15*, 7408−7440.
(15) Sultan, S.; Crovetto, L.; Rios, R. Recent advances in the development of enantiopure BODIPYs and some related enantiomeric compounds. *Chem. Commun.* **2025**, *61*, 1989−2010.
(16) Sánchez-Carnerero, E. M.; Moreno, F.; Maroto, B. L.; Agarrabeitia, A. R.; Ortiz, M. J.; Vo, B. G.; Muller, G.; de la Moya, S. Circularly Polarized Luminescence by Visible-Light Absorption in a Chiral O-BODIPY Dye: Unprecedented Design of CPL Organic Molecules from Achiral Chromophores. *J. Am. Chem. Soc.* **2014**, *136*, 3346−3349.
(17) Bruhn, T.; Pescitelli, G.; Jurinovich, S.; Schaumlöffel, A.; Witterauf, F.; Ahrens, J.; Bröring, M.; Bringmann, G. Axially Chiral BODIPY DYEmers: An Apparent Exception to the Exciton Chirality Rule. *Angew. Chem., Int. Ed.* **2014**, *53*, 14592−14595.
(18) Maeda, C.; Suka, K.; Nagahata, K.; Takaishi, K.; Ema, T. Synthesis and Chiroptical Properties of Chiral Carbazole-Based BODIPYs. *Chem.—Eur. J.* **2020**, *26*, 4261−4268.
(19) Cao, J.; Zhang, J.-P.; Zhang, F.; Kang, Z.; Jiao, L.; Li, Z.-Y.; Hao, E. A. Catalytic Enantioselective Suzuki Coupling for the Modular Construction of Axially Chiral BODIPYs with Bright Solid-State Emission. *Org. Lett.* **2025**, *27*, 173−179.
(20) Guerrero-Corella, A.; Asenjo-Pascual, J.; Pawar, T. J.; Díaz-Tendero, S.; Martín-Sómer, A.; Gómez, C. V.; Belmonte-Vázquez, J. L.; Ramírez-Ornelas, D. E.; Peña-Cabrera, E.; Fraile, A.; Cruz, D. C.; Alemán, J. BODIPY as electron withdrawing group for the activation of double bonds in asymmetric cycloaddition reactions. *Chem. Sci.* **2019**, *10*, 4346−4351.
(21) Díaz-Norambuena, C.; Ray, C.; Arbeloa, T.; Oliden-Sánchez, A.; Moreno, F.; Maroto, B. L.; Bañuelos, J.; de la Maya, S. Bridge-induced taming of the visible electronic circular dichroism signatures of helicoBODIPYs. *Dyes Pigm.* **2024**, *222*, 111907.
(22) Ito, H.; Sakai, H.; Suzuki, Y.; Kawamata, J.; Hasobe, T. Systematic Control of Structural and Photophysical Properties of π-Extended Mono- and Bis-BODIPY Derivatives. *Chem.—Eur. J.* **2020**, *26*, 316−325.
(23) Maeda, C.; Nagahata, K.; Shirakawa, T.; Ema, T. Azahelicene-Fused BODIPY Analogues Showing Circularly Polarized Luminescence. *Angew. Chem., Int. Ed.* **2020**, *59*, 7813−7817.
(24) Li, X.; Zhang, G.; Song, Q. Recent advances in the construction of tetracoordinate boron compounds. *Chem. Commun.* **2023**, *59*, 3812−3820.
(25) Abdou-Mohamed, A.; Aupic, C.; Fournet, C.; Parrain, J. L.; Chouraqui, G.; Chuzel, O. Stereoselective formation of boron-stereogenic organoboron derivatives. *Chem. Soc. Rev.* **2023**, *52*, 4381−4391.
(26) Zu, B.; Guo, Y.; He, C. Catalytic Enantioselective Construction of Chiroptical Boron-Stereogenic Compounds. *J. Am. Chem. Soc.* **2021**, *143*, 16302−16310.
(27) Zhang, G.; Zhang, Z.; Hou, M.; Cai, X.; Yang, K.; Yu, P.; Song, Q. Construction of boron-stereogenic compounds via enantioselective Cu-catalyzed desymmetric B−H bond insertion reaction. *Nat. Commun.* **2022**, *13*, 2624.
(28) Zu, B.; Guo, Y.; Ren, L.-Q.; Li, Y.; He, C. Catalytic enantioselective synthesis of boron-stereogenic BODIPYs. *Nat. Synth.* **2023**, *2*, 564−571.
(29) Ren, L.-Q.; Zhan, B.; Zhao, J.; Guo, Y.; Zu, B.; Li, Y.; He, C. Modular enantioselective assembly of multi-substituted boron-stereogenic BODIPYs. *Nat. Chem.* **2025**, *17*, 83−91.
(30) Zhan, B.; Ren, L.-Q.; Zhao, J.; Zhang, H.; He, C. Catalytic Asymmetric C−N Cross-Coupling towards Boron-Stereogenic 3-Amino-BODIPYs. *Nat. Commun.* **2025**, *16*, 438.
(31) Gao, Y.; Liu, Z.; Tian, S.; Min, Y.; Li, X.; Chen, Y.; Hong, X.; Zhang, W.; Wang, L. Catalytic Enantioselective Synthesis of Boron-Stereogenic and Axially Chiral BODIPYs via Rhodium(II)-Catalyzed C−H (Hetero) Arylation with Diazonaphthoquinones and Diazoindenines. *Angew. Chem., Int. Ed.* **2024**, *64*, No. e202418888.
(32) Maruoka, K.; Ooi, T. Enantioselective Amino Acid Synthesis by Chiral Phase-Transfer Catalysis. *Chem. Rev.* **2003**, *103*, 3013−3028.
(33) Ooi, T.; Maruoka, K. Recent Advances in Asymmetric Phase-Transfer Catalysis. *Angew. Chem., Int. Ed.* **2007**, *46*, 4222−4266.
(34) Hashimoto, T.; Maruoka, K. Recent Development and Application of Chiral Phase-Transfer Catalysts. *Chem. Rev.* **2007**, *107*, 5656−5682.
(35) Brak, K.; Jacobsen, E. N. Asymmetric Ion-Pairing Catalysis. *Angew. Chem., Int. Ed.* **2013**, *52*, 534−561.
(36) Shirakawa, S.; Maruoka, K. Recent Developments in Asymmetric Phase-Transfer Reactions. *Angew. Chem., Int. Ed.* **2013**, *52*, 4312−4348.
(37) Proctor, R. S. J.; Colgan, A. C.; Phipps, R. J. Exploiting attractive non-covalent interactions for the enantioselective catalysis of reactions involving radical intermediates. *Nat. Chem.* **2020**, *12*, 990−1004.
(38) Schirmer, T. E.; König, B. Ion-Pairing Catalysis in Stereoselective, Light-Induced Transformations. *J. Am. Chem. Soc.* **2022**, *144*, 19207−19218.
(39) Lee, H. J.; Maruoka, K. Asymmetric phase-transfer catalysis. *Nat. Rev. Chem* **2024**, *8*, 851−869.
(40) Islas-Gonzalez, G.; Bois-Choussy, M.; Zhu, J. From central to planar chirality, the first example of atropenantioselective cycloetherification. *Org. Biomol. Chem.* **2003**, *1*, 30−32.
(41) Bella, M.; Kobbelgaard, S.; Jørgensen, K. A. Organocatalytic Regio- and Asymmetric C-Selective S_NAr ReactionsStereoselective Synthesis of Optically Active Spiro-pyrrolidone-3,3′-oxoindoles. *J. Am. Chem. Soc.* **2005**, *127*, 3670−3671.
(42) Kobbelgaard, S.; Bella, M.; Jørgensen, K. A. Improved Asymmetric S_NAr Reaction of β-Dicarbonyl Compounds Catalyzed by Quaternary Ammonium Salts Derived from Cinchona Alkaloids. *J. Org. Chem.* **2006**, *71*, 4980−4987.
(43) Shirakawa, S.; Koga, K.; Tokuda, T.; Yamamoto, K.; Maruoka, K. Catalytic Asymmetric Synthesis of 3,3′-Diaryloxindoles as Triarylmethanes with a Chiral All-Carbon Quaternary Center: Phase-Transfer-Catalyzed S_NAr Reaction. *Angew. Chem., Int. Ed.* **2014**, *53*, 6220−6223.
(44) Shirakawa, S.; Yamamoto, K.; Tokuda, T.; Maruoka, K. Phase-Transfer-Catalyzed Asymmetric α-Arylation of α-Amino Acid Derivatives. *Asian J. Org. Chem.* **2014**, *3*, 433−436.
(45) Shirakawa, S.; Yamamoto, K.; Maruoka, K. Phase-Transfer-Catalyzed Asymmetric S_NAr Reaction of α-Amino Acid Derivatives with Arene Chromium Complexes. *Angew. Chem., Int. Ed.* **2015**, *54*, 838−840.
(46) Ding, Q.; Wang, Q.; He, H.; Cai, Q. Asymmetric Synthesis of (−)-Pterocarine and (−)-Galeon via Chiral Phase Transfer-Catalyzed Atropselective Formation of Diarylether Cyclophane Skeleton. *Org. Lett.* **2017**, *19*, 1804−1807.
(47) Guo, F.; Fang, S.; He, J.; Su, Z.; Wang, T. Enantioselective organocatalytic synthesis of axially chiral aldehyde-containing styrenes via S_NAr reaction-guided dynamic kinetic resolution. *Nat. Commun.* **2023**, *14*, 5050.
(48) Hu, H.-L.; Fang, S.; Luo, X.; He, J.; Wu, J.-H.; Su, Z.; Xu, Z.; Wang, T. Organocatalytic Enantioselective Arylation to Access Densely Aryl-Substituted P-Stereogenic Centers. *Org. Lett.* **2025**, *27*, 109−114.
(49) Piers, W. E.; Chivers, T. Pentafluorophenylboranes: from obscurity to applications. *Chem. Soc. Rev.* **1997**, *26*, 345−354.
(50) Sivaev, I. B.; Bregadze, V. I. *Coord. Chem. Rev.* **2014**, *270*, 75−88.
(51) Paradies, J. Metal-Free Hydrogenation of Unsaturated Hydrocarbons Employing Molecular Hydrogen. *Angew. Chem., Int. Ed.* **2014**, *53*, 3552−3557.
(52) Oestreich, M.; Hermeke, J.; Mohr, J. A unified survey of Si−H and H−H bond activation catalysed by electron-deficient boranes. *Chem. Soc. Rev.* **2015**, *44*, 2202−2220.
(53) Carden, J. L.; Dasgupta, A.; Melen, R. L. Halogenated triarylboranes: synthesis, properties and applications in catalysis. *Chem. Soc. Rev.* **2020**, *49*, 1706−1725.
(54) Fang, H.; Oestreich, M. Defunctionalisation catalysed by boron Lewis acids. *Chem. Sci.* **2020**, *11*, 12604−12615.
(55) Zhou, X.; Yu, C.; Feng, Z.; Yu, Y.; Wang, J.; Hao, E.; Wei, Y.; Mu, X.; Jiao, L. Highly Regioselective α-Chlorination of the BODIPY

Chromophore with Copper(II) Chloride. *Org. Lett.* **2015**, *17*, 4632−4635.
(56) Dai, E.; Pang, W.; Zhang, X.-F.; Yang, X.; Jiang, T.; Zhang, P.; Yu, C.; Hao, E.; Wei, Y.; Mu, X.; Jiao, L. Synthesis and Photophysics of BF2-Rigidified Partially Closed Chain Bromotetrapyrroles: Near Infrared Emitters and Photosensitizers. *Chem.—Asian J.* **2015**, *10*, 1327−1334.
(57) Climent, E.; Biyikal, M.; Gawlitza, K.; Dropa, T.; Urban, M.; Costero, A. M.; Martínez-Máñez, R.; Rurack, K. A. A Rapid and Sensitive Strip-Based Quick Test for Nerve Agents Tabun, Sarin, and Soman Using BODIPY-Modified Silica Materials. *Chem.—Eur. J.* **2016**, *22*, 11138−11142.
(58) Satoh, T.; Fujii, K.; Kimura, Y.; Matano, Y. Synthesis of 3,5-Disubstituted BODIPYs Bearing N-Containing Five-Membered Heteroaryl Groups via Nucleophilic C−N Bond Formation. *J. Org. Chem.* **2018**, *83*, 5274−5281.
(59) Wang, L.; Cheng, C.; Li, Z.-Y.; Guo, X.; Wu, Q.; Hao, E.; Jiao, L. Nucleophilic Aromatic Substitution (S_NAr) as an Approach to Challenging Nitrogen-Bridged BODIPY Oligomers. *Org. Lett.* **2024**, *26*, 3026−3031.
(60) Bu, Y.; Rong, M.; Wang, J.; Zhu, X.; Zhang, J.; Wang, L.; Yu, Z.; Tian, Y.; Zhou, H.; Xie, Y. Cancer Cell Membrane Labeling Fluorescent Doppelganger Enables In Situ Photoactivated Membrane Dynamics Tracking via Two-Photon Fluorescence Imaging Microscopy. *Anal. Chem.* **2022**, *94*, 8373−8381.
(61) Ren, S.; Liu, Z.; Li, P.; Liu, H.; Lu, M.; Wang, K.; Yao, J.; Dong, H.; Yang, Q.-Z.; Zhao, Y. S. Circularly Polarized Lasing from Helical Superstructures of Chiral Organic Molecules. *Angew. Chem., Int. Ed.* **2024**, *64*, No. e202415092.
(62) Aknine, N.; Klymchenko, A. S. Push−Pull Fluorescent Dyes with Trifluoroacetyl Acceptor for High-Fidelity Sensing of Polarity and Heterogeneity of Lipid Droplets. *Anal. Chem.* **2024**, *96*, 13242−21325.
(63) Wu, X.; Wang, X.-X.; Li, Y.; Kong, F.; Xu, K.; Li, L.; Tang, B. A Near-Infrared Probe for Specific Imaging of Lipid Droplets in Living Cells. *Anal. Chem.* **2022**, *94*, 4881−4888.
(64) Huang, H.; Bu, Y.; Yu, Z.; Rong, M.; Li, R.; Wang, Z.; Zhang, J.; Zhu, X.; Wang, L.; Zhou, H. Solvatochromic Two-Photon Fluorescent Probe Enables In Situ Lipid Droplet Multidynamics Tracking for Nonalcoholic Fatty Liver and Inflammation Diagnoses. *Anal. Chem.* **2022**, *94*, 13396−13403.
(65) Kim, E. S.; Lee, J. M.; Kwak, J. Y.; Lee, H. W.; Lee, I. J.; Kim, H. M. Multicolor Two-Photon Microscopy Imaging of Lipid Droplets and Liver Capsule Macrophages In Vivo. *Anal. Chem.* **2024**, *96*, 8467−8473.

https://doi.org/10.1021/jacsau.5c00196
JACS Au 2025, 5, 1965−1973